Journal of Microbiology (2022) Vol. 60, No. 5, pp. 469–477
DOI 10.1007/s12275-022-1647-5
eISSN 1976-3794
pISSN 1225-8873

# *Lysobacter ciconiae* sp. nov., and *Lysobacter avium* sp. nov., isolated from the faeces of an Oriental stork[§]

**So-Yeon Lee[1], Pil Soo Kim[2], Hojun Sung[2], Dong-Wook Hyun[1], and Jin-Woo Bae[1,2*]**

[1]*Department of Biology and Department of Biomedical and Pharmaceutical Sciences, Kyung Hee University, Seoul 02447, Republic of Korea*
[2]*Department of Life and Nanopharmaceutical Sciences and Department of Biology, Kyung Hee University, Seoul 02447, Republic of Korea*

(Received Dec 15, 2021 / Revised Feb 9, 2022 / Accepted Feb 11, 2022)

**Two Gram-stain-negative, mesophilic, strictly aerobic, non-spore forming, and yellow-pigmented strains with rod-shaped cells, designated H21R20$^T$ and H23M41$^T$, were isolated from the faeces of an Oriental stork (*Ciconia boyciana*). Based on 16S rRNA gene sequences, both strains showed the highest similarity (98.3–98.4%) to the type strain of *Lysobacter concretionis*. Phylogenetic analysis based on the 16S rRNA genes and 92 bacterial core genes showed that strains H21R20$^T$ and H23M41$^T$ were robustly clustered with *L. concretionis* Ko07$^T$. Whole genome sequencing revealed that the genomes of both strains were approximately 2.9 Mb in size. The DNA G + C contents of the H21R20$^T$ and H23M41$^T$ strains were 67.3 and 66.6%, respectively. The two strains showed 80.1–81.7% average nucleotide identity with *L. concretionis* Ko07$^T$. Strain H21R20$^T$ grew optimally at 30°C and pH 8.0 and in the presence of 0.5–3% (wt/vol) NaCl, while strain H23M41$^T$ grew optimally at 30°C and pH 7.0–8.0 and in the presence of 0–3% (wt/vol) NaCl. Both strains possessed iso-$C_{15:0}$, iso-$C_{16:0}$ and summed feature 9 (iso-$C_{17:1}$ $\omega$9c and/or $C_{16:0}$ 10-methyl) as the major cellular fatty acids, ubiquinone Q-8 as a predominant quinone, and diphosphatidylglycerol, phosphatidylglycerol, and phosphatidylethanolamine as the major polar lipids. A multifaceted investigation demonstrated that strains H21R20$^T$ and H23M41$^T$ represent novel species of the genus *Lysobacter*, for which we propose the names *Lysobacter ciconiae* sp. nov. and *Lysobacter avium* sp. nov. for strains H21R20$^T$ (= KCTC 82316$^T$ = JCM 34832$^T$) and H23M41$^T$ (= KCTC 62676$^T$ = JCM 33223$^T$), respectively.**

***Keywords***: *Lysobacter*, *Lysobacter ciconiae*, *Lysobacter avium*, Oriental stork, *Ciconia boyciana*

*For correspondence. E-mail: baejw@khu.ac.kr; Tel.: +82-2-961-2312; Fax: +82-2-961-9155
[§]Supplemental material for this article may be found at https://doi.org/10.1007/s12275-022-1647-5.


## Introduction

The genus *Lysobacter* belongs to the family *Lysobacteraceae*, order *Lysobacterales*, class *Gammaproteobacteria*, and phylum *Pseudomonadota* (Christensen and Cook, 1978). This genus currently contains 65 valid published species names (https://lpsn.dsmz.de/genus/lysobacter) (Parte *et al.*, 2020), with *Lysobacter enzymogenes* as the type species (Christensen and Cook, 1978). The members of this genus are Gram-stain-negative and aerobic rods with predominance of iso-branched fatty acids. They contain ubiquinone Q-8 as the major respiratory quinone and diphosphatidylglycerol (DPG), phosphatidylglycerol (PG), and phosphatidylethanolamine (PE) as the major polar lipids. Their genome size and DNA G + C content range from 2.5 to 6.7 Mb and 61.6 to 71.6%, respectively (Christensen and Cook, 1978; Ten *et al.*, 2008; Du *et al.*, 2015; Choi *et al.*, 2018; Huo *et al.*, 2018; Jang *et al.*, 2018; Margesin *et al.*, 2018; Xiao *et al.*, 2019; Kim *et al.*, 2021). Most members of this genus have been isolated from various terrestrial samples, including park, field, farmland, forest, mountain, plateau meadow, plant cultivation, and greenhouse soils, and the plant rhizosphere (Zhang *et al.*, 2011, 2019; Du *et al.*, 2015; Singh *et al.*, 2015a, 2015b; Kim *et al.*, 2016, 2017, 2019, 2021; Lee *et al.*, 2017; Huo *et al.*, 2018; Jang *et al.*, 2018; Margesin *et al.*, 2018; Luo *et al.*, 2019; Xiao *et al.*, 2019; Fang *et al.*, 2020; Li *et al.*, 2020; Ten *et al.*, 2020) and watery samples, including activated sludge, freshwater, lake, stream, and estuary sediments, sea water, and sponging (Ten *et al.*, 2008; Ye *et al.*, 2015; Jeong *et al.*, 2016; Siddiqi and Im, 2016; Choi *et al.*, 2018; Chhetri *et al.*, 2019; Im *et al.*, 2020; Xu *et al.*, 2021). However, unlike the previous cases, in this study, we isolated two putative novel strains belonging to the genus *Lysobacter*, designated H21R20$^T$ and H23M41$^T$, from the faeces of the Oriental stork. We analyzed their taxonomic positions and polyphasic characteristics.

## Materials and Methods

### Bacterial isolation and deposition

We obtained a fecal sample of an Oriental stork from the Seoul Grand Park Zoo and diluted this sample ($10^{-2}$) using sterile phosphate-buffered saline. The diluted suspension was spread onto plates containing tryptic soy broth (TSB, Bacto) and marine broth (MB, Difco) with 1.5% agar (TSA and MA) and Reasoner's 2A agar (R2A, Difco). Colonies were collected from agar plates incubated at 10°C and 30°C and pure colonies were stored at -80°C in 40% (vol/vol) glycerol stocks. The representative isolates were deposited at the Korean Collection for Type Cultures (KCTC) and the Japan Collection

of Microorganisms (JCM). The accession numbers are KCTC 82316 and JCM 34832 for strain H21R20$^T$ and KCTC 62676 and JCM 33223 for strain H23M41$^T$.

### Phylogenetic and genomic analyses

We extracted the genomic DNA using the QIAamp Fast DNA Stool Mini Kit (Qiagen) and sequenced the DNA samples using the 27F, 785F, 800R, and 1492R primers (Lane, 1991). We assembled the sequence fragments using the SeqMan 5.0 software program (DNASTAR) and aligned the sequences with 16S rRNA gene sequences of closely related species using CLUSTAL W software (Thompson *et al.*, 1994). We constructed a phylogenetic consensus tree using the MEGA (version 7.0.26) program (Kumar *et al.*, 2016) with 1,000 bootstrap replicates. To ascertain phylogenetic position of the two strains, the phylogenetic tree was constructed using the neighbor-joining (NJ), maximum-likelihood (ML), and maximum-parsimony (MP) algorithms (Kluge and Farris, 1969; Felsenstein, 1981; Saitou and Nei, 1987) with regard to closely related strains in the genus *Lysobacter*. *Rhodanobacter lindaniclasticus* RP5557$^T$ was used as an outgroup. Complete genome sequences were obtained by PacBio RS II sequencing (DNA link Inc.) and assembled *de novo* using the Hierarchical Genome Assembly Process (HGAP, version 3.0) (Chin *et al.*, 2013). To further confirm the phylogenomic position of the isolates in the genus *Lysobacter*, we constructed an up-to-date bacterial core gene (UBCG) tree (Na *et al.*, 2018) with closely related strains using the FastTree program (Price *et al.*, 2009). The overall genome-related indices (OGRIs) (Chun *et al.*, 2018) were also calculated. The original average nucleotide identity (ANI) and orthologous ANI (OrthoANI) values were calculated using the OAT program on the EzBioCloud server (https://www.ezbiocloud.net/) (Lee *et al.*, 2016) and the digital DNA-DNA hybridization (dDDH) values were calculated using the genome-to-genome distance calculator (GGDC) 2.1 (http://ggdc.dsmz.de/) (Meier-Kolthoff *et al.*, 2013). The pan-genome analysis was performed using an app named Build Pangenome with OrthoMCL (version 2.0) (Li *et al.*, 2003) on the KBase server (https://www.kbase.us/) (Arkin *et al.*, 2018). Genes found in all input genomes were classified as 'core' genes, single genes found in only one genome were classified as 'singleton' genes, and the other genes were classified as 'accessory' genes. The genes were grouped into subsystems and clusters of orthologous groups (COGs) using the rapid annotation using subsystem technology (RAST) server (https://rast.nmpdr.org/) and the IMG-Expert Review (IMG-ER) platform (https://img.jgi.doe.gov/), respectively (Brettin *et al.*, 2015; Chen *et al.*, 2019). The virulence factor (VF) genes encoding toxins were searched using the TrueBac ID service (https://www.truebacid.com/) (Ha *et al.*, 2019). The VF database (VFDB) IDs are obtained from the Virulence factor database (http://www.mgc.ac.cn/VFs/main.htm). Carbohydrate-active enzymes (CAZymes) were annotated using HMMER, DIAMOND, Hotpep, and CAZyme gene cluster (CGC) Finder on the database for automated CAZyme annotation (dbCAN) meta server (http://bcb.unl.edu/dbCAN2/index.php) (Zhang *et al.*, 2018). Genomic regions comprising at least one CAZyme gene, one transporter (TC) gene, and one transcription factor (TF) gene were defined as CGCs.

### Phenotypic characterization

To discover the optimum conditions for the growth of the strains, we cultured the strains under diverse temperatures (4, 10, 15, 20, 25, 30, 37, 45, 55, and 65°C), NaCl concentrations (0, 0.5, 1, 1.5, 2, 3, 4, 5, 6, 7, 8, 10, and 12%, wt/vol), and pH (4, 5, 6, 7, 8, 9, 10, 11 pH) in TSB and measured the turbidity of the cultures at 600 nm using a Synergy Mx spectrophotometer (BioTek) after 1, 2, and 7 days of incubation (Lee *et al.*, 2020). We also tested the oxygen dependence of the strains by culturing them in an anaerobic chamber under $N_2$ (90%), $H_2$ (5%), and $CO_2$ (5%) for 7 days. We performed Gram staining and spore formation analyses using a Gram staining kit (bioMérieux) and the malachite green staining method, respectively, and observed using an light microscope (Eclipse 50i; Nikon) (Schaeffer and Fulton, 1933). Morphological features were observed under an energy-filtering transmission electron microscope (LIBRA 120; Zeiss) after two days of incubation. Cellular motility was tested using semi-solid TSB with 0.4% agar (Lee *et al.*, 2019). The API 20NE and API ZYM strips (bioMérieux), and the GEN III MicroPlate (Biolog) were used for testing the enzyme activities and utilization of carbon sources. We further tested catalase and oxidase activities by observing bubble production in the presence of 3% (vol/vol) hydrogen peroxide solution and indophenol blue after adding 1% (wt/vol) tetramethyl *p*-phenylenediamine solution (bioMérieux), respectively (Hyun *et al.*, 2021). The susceptibility of the strains to 28 different types of antibiotics was tested. The discs (Bio-Rad) containing the following antibiotics were used: 2 μg (clindamycin), 5 μg (ciprofloxacin, moxifloxacin, levofloxacin, rifampicin, and trimethoprim), 10 μg (ampicillin, colistin, ertapenem, gentamicin, imipenem, norfloxacin, and streptomycin), 15 μg (azithromycin, clarithromycin, erythromycin, and tigecycline), 30 μg (aztreonam, cefepime, cefoxitin, ceftriaxone, cephalothin, chloramphenicol, kanamycin, tetracycline, and vancomycin), 100 μg (carbenicillin), and 300 μg (polymixin). We spread the cell suspensions and placed the discs onto TSA plates. The plates were incubated at 30°C for two days and the radius of the growth-inhibition zones was measured. The susceptibilities were scored as follows: resistant, moderately susceptible, susceptible, and hypersusceptible if the radius was less than 1 mm, 1–5 mm, greater than 5 mm, and greater than 2 cm, respectively.

### Chemotaxonomic analyses

We extracted the cellular fatty acids following the protocol described in the Sherlock Microbial Identification System (MIDI) operating manual (version 4.5) and separated them using gas chromatography (6890 GC system; Agilent). The Microbial Identification software package (Sherlock version 6.3) based on the TSBA6 library (Sasser, 1990) was used for the identification of the fatty acids. Polar lipids were also extracted from freeze-dried cell harvests in accordance with previously described methods (Minnikin *et al.*, 1984). For two-dimensional thin-layer chromatography (TLC) analysis, two types of solvents were used for separation and four types of spray reagents were used for detection. A mixture of chloroform:methanol:distilled water (DW) (65:25:4, vol/vol/vol) and a mixture of chloroform:acetic acid:methanol:DW

(80:15:12:4, vol/vol/vol/vol) were used for the first and the second dimension, respectively. Next, 5% (wt/vol) ethanolic molybdatophosphoric acid and ninhydrin spray reagent (Sigma-Aldrich) were used for total lipid and aminolipid (AL) detection, while molybdenum blue spray reagent (Sigma-Aldrich) and $\alpha$-naphthol-sulfuric acid reagent were used for phospholipid (PL) and glycolipid (GL) detection, respectively (Lee *et al.*, 2021). For quinone analysis, cell harvesting and extraction were performed in the absence of light and a mixture of chloroform/methanol (2:1, vol/vol) was used for the extraction process (Collins and Jones, 1981). The extracted quinones were identified using a reversed phase–high performance liquid chromatography (RP–HPLC) instrument (Younglin) (Hiraishi *et al.*, 1996).

## Comparative analyses

We obtained *L. concretionis* Ko07$^T$ from the KCTC and compared various phenotypic characteristics of this strain with those of the strains H21R20$^T$ and H23M41$^T$. We also obtained the API data and cellular fatty acid profiles of *L. enzymogenes* 495$^T$, the type strain of *Lysobacter*, for comparative analysis (Srinivasan *et al.*, 2010). Genome sequences of *L. concretionis* Ko07$^T$ and *L. enzymogenes* 495$^T$ were obtained from NCBI database.

## Accession numbers

The DDBJ/ENA/GenBank accession numbers for the 16S rRNA gene sequences of strains H21R20$^T$ and H23M41$^T$ are

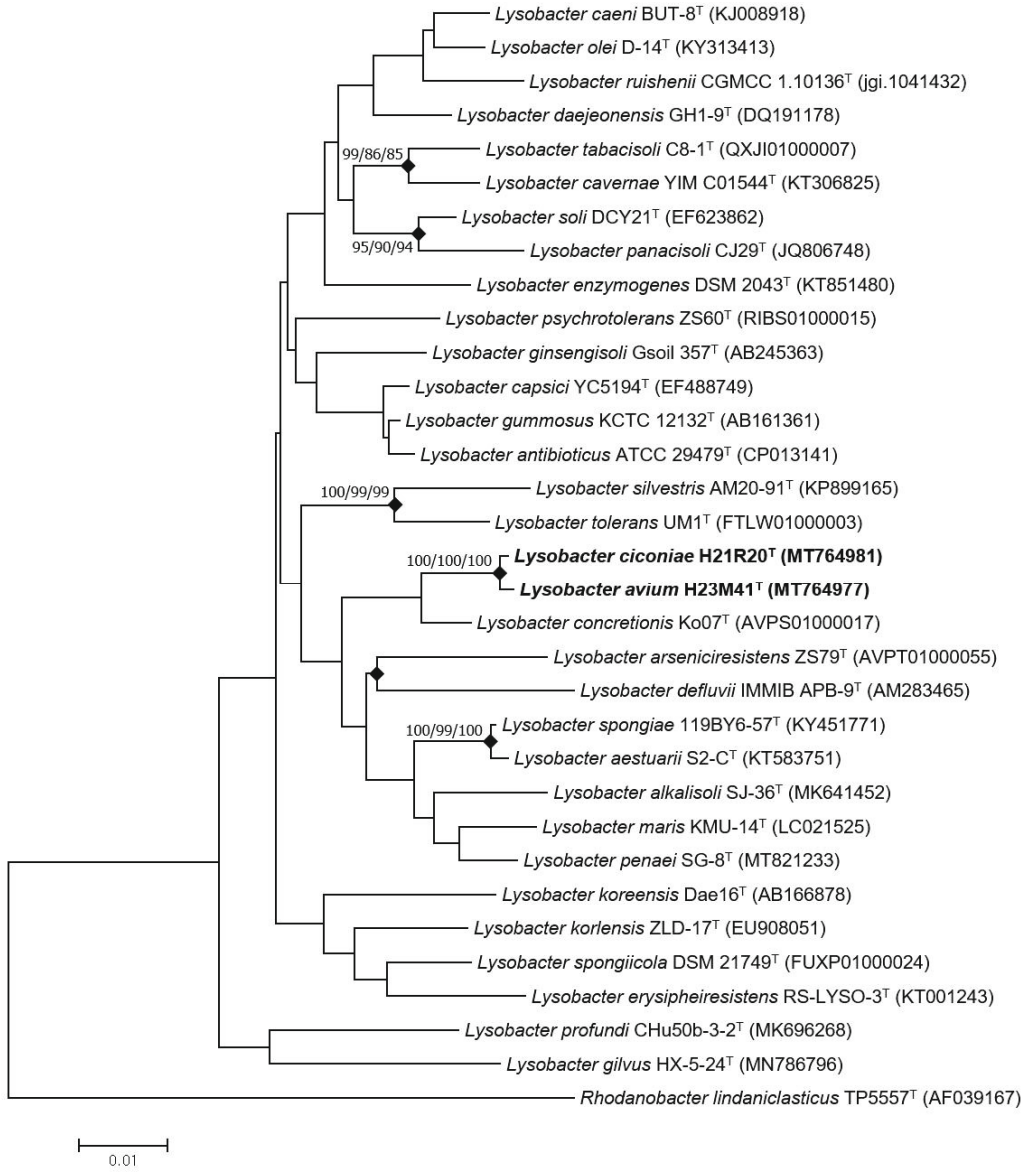


**Fig. 1. The phylogenetic tree of strains H21R20$^T$ and H23M41$^T$ and closely related *Lysobacter* species.** A phylogenetic tree based on the 16S rRNA gene sequences was constructed using NJ, ML, and MP algorithms and 1,000 re-samplings were performed. The equivalent nodes of the NJ, ML, and MP algorithms are marked with filled diamonds and the bootstrap values (NJ/ML/MP) are presented at the nodes. *Rhodanobacter lindaniclasticus* TP5557$^T$ was selected as an outgroup. Bar, 0.01 substitution per nucleotide position.

MT764981 and MT764977, respectively. The DDBJ/ENA/GenBank accession numbers for the whole-genome sequences of strains H21R20$^T$ and H23M41$^T$ are CP063656 and CP063657, respectively.

## Results and Discussion

### Phylogenetic and genomic analyses

Based on the 16S rRNA gene sequences, strains H21R20$^T$ and H23M41$^T$ were identified to be affiliated with the genus *Lysobacter*, the family *Lysobacteraceae*, the order *Lysobacterales*, the class *Gammaproteobacteria*, the phylum *Pseudomonadota*. In a phylogenetic tree constructed with 16S rRNA gene sequences, the two strains formed a monophyletic clade with *L. concretionis* Ko07$^T$, with which they showed the highest sequence similarity (98.3–98.4%) (Fig. 1). Similarly, in a UBCG tree constructed using genome sequences, the two strains were grouped again with *L. concretionis* Ko07$^T$ (Fig. 2), suggesting that strains H21R20$^T$ and H23M41$^T$ were affiliated to the genus *Lysobacter*.

To confirm the two strains as new members of the genus *Lysobacter*, we compared three types of OGRI indices. Strain H21R20$^T$ and strain H23M41$^T$ showed 81.1% and 80.1% original ANI values, respectively, 81.7% and 80.7% OrthoANI values, respectively and 24.9% and 24.0% dDDH values, respectively, compared with *L. concretionis* Ko07$^T$ (Supplementary data Table S1). These values were well below the species classification thresholds (95–96% for ANI and 70% for dDDH values) (Chun *et al.*, 2018), suggesting that strains H21R20$^T$ and H23M41$^T$ be proposed as two novel species of the genus *Lysobacter*.

The genome of the strains H21R20$^T$ and H23M41$^T$ contained 2,914,291 bp with 67.3% DNA G + C content and 2,854,808 bp with 66.6% DNA G + C content, respectively. The genomes of both strains were of a relatively small size, considering that the genome sizes of other members of the genus *Lysobacter* range from 2.5 to 6.7 Mb. The strains H21R20$^T$ and H23M41$^T$ harbored a total of 2,647 and 2,591 genes, respectively, and 50 and 49 tRNA genes, respectively. Both these strains harbored two 5S, two 16S, and two 23S rRNA genes (Table 1).

Protein-coding genes were classified as core, accessory, and

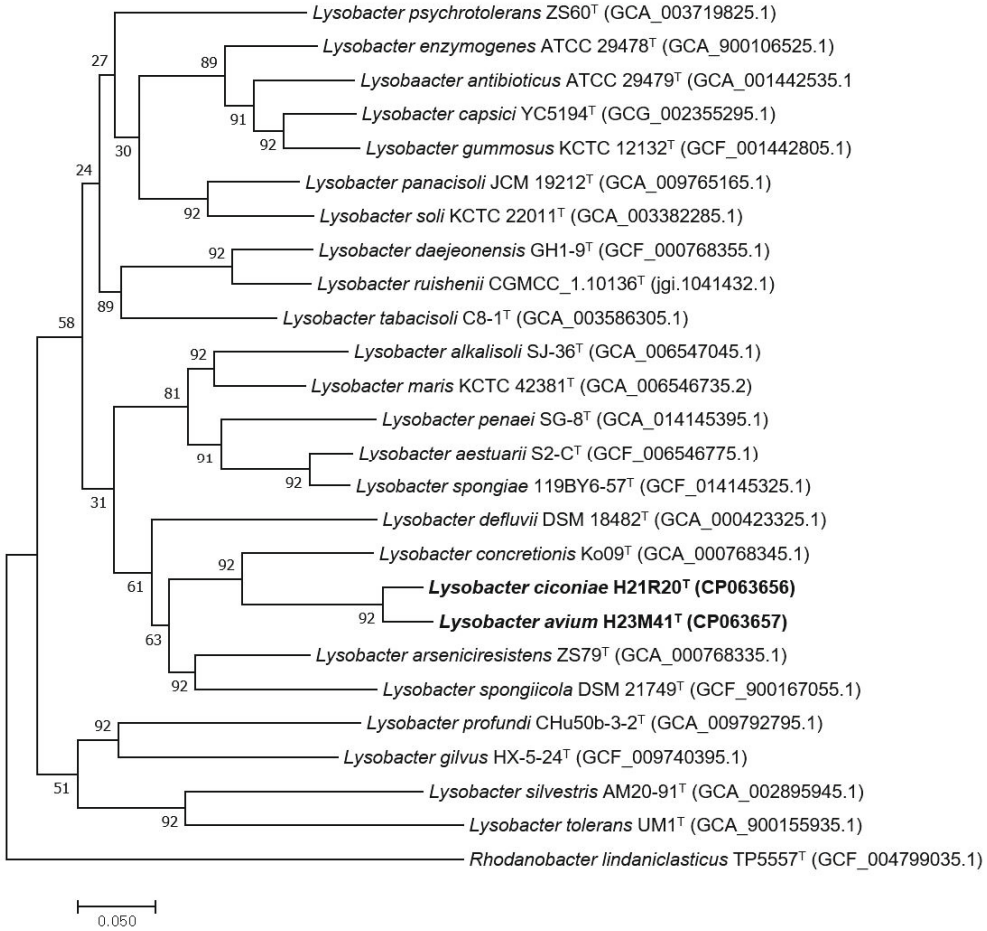


**Fig. 2. The UBCG tree of strains H21R20$^T$ and H23M41$^T$ and closely related *Lysobacter* species.** The numbers presented on the nodes represent the gene support index, which is the number of single gene trees supporting the branch. *Rhodanobacter lindaniclasticus* TP5557$^T$ was used as an outgroup. Bar, 0.05 substitution per nucleotide.

**Table 1.** **The genomic features of strain H21R20$^T$, strain H23M41$^T$, *L. concretionis* Ko07$^T$, and *L. enzymogenes* 495$^T$**
Strains: 1, strain H21R20$^T$; 2, strain H23M41$^T$; 3, *L. concretionis* Ko07$^T$; 4, *L. enzymogenes* 495$^T$.

| Strain | Size | Contig | G + C (%) | Gene number | rRNA (5S/16S/23S) | tRNA | Accession number |
|---|---|---|---|---|---|---|---|
| 1 | 2,914,291 | 1 | 67.3 | 2647 | 6 (2/2/2) | 50 | CP063656 |
| 2 | 2,854,808 | 1 | 66.6 | 2591 | 6 (2/2/2) | 49 | CP063657 |
| 3 | 3,032,117 | 26 | 67.3 | 2685 | 3 (1/1/1) | 46 | AVPS01 |
| 4 | 6,263,953 | 23 | 69.2 | 5091 | 5 (3/1/1) | 54 | FNOG01 |

singleton genes by pan-genome analysis. Strain H21R20$^T$, strain H23M41$^T$, and *L. concretionis* Ko07$^T$ shared 1,908 homolog gene families. Strains H21R20$^T$ and H23M41$^T$ shared 2,070 and 1,967 homolog gene families, respectively, with *L. concretionis* Ko07$^T$. Strain H21R20$^T$, strain H23M41$^T$, and *L. concretionis* Ko07$^T$ harbored 1,923 (75.9%), 1,926 (81.8%), and 1,933 (71.2%) core genes, respectively. Strain H21R20$^T$, strain H23M41$^T$, and *L. concretionis* Ko07$^T$ contained 142 (5.6%), 174 (7.4%), and 409 (15.1%) singleton genes, respectively (Supplementary data Table S2 and Fig. S1). Strain H21R20$^T$ and strain H23M41$^T$ shared the largest number of homolog gene families, followed by strain H21R20$^T$ and *L. concretionis* Ko07$^T$. Strain H23M41$^T$ and *L. concretionis* Ko07$^T$ shared the smallest number of homolog gene families and *L. concretionis* Ko07$^T$ contained the largest number of singleton genes among the three strains (Supplementary data Table S2 and Fig. S1). These results correspond to the comparisons of OGRI indices (Supplementary data Table S1), suggesting that strain H21R20$^T$ and strain H23M41$^T$ shared relatively similar genomic features compared to *L. concretionis* Ko07$^T$. Strain H21R20$^T$ was more genomically related to *L. concretionis* Ko07$^T$ than strain H23M41$^T$ was to *L. concretionis* Ko07$^T$.

The genes were grouped into several subsystems and assigned to COG functional categories. The major subsystems associated with the three strains were 'cofactors, vitamins, prosthetic groups, pigments', 'membrane transport', 'protein metabolism', 'DNA metabolism', 'respiration', 'amino acids and derivatives', and 'carbohydrates'. Strain H21R20$^T$ contained lower proportion of subsystems related to 'fatty acids, lipids, and isoprenoids' than the other strains. *Lysobacter concretionis* Ko07$^T$ harbored lower proportion of subsystems related to 'nitrogen metabolism' than the other strains (Supplementary data Table S3). The major COGs were amino acid transport and metabolism (code E), cell wall/membrane/envelope biogenesis (M), and energy production and conversion (C). Strain H23M41$^T$ harbored the lowest number of genes related to cell motility (N). *Lysobacter concretionis* Ko07$^T$ contained a lower proportion of genes related to amino acid transport and metabolism (E), carbohydrate transport and metabolism (G), cell wall/membrane/envelope biogenesis (M), inorganic ion transport and metabolism (P), posttranslational modification, protein turnover, chaperones (O), and transcription (K) than the other strains (Supplementary data Table S4).

Thirty VF-like genes were common among all the compared strains. Strains H21R20$^T$ and H23M41$^T$ harbored 77 and 38 VF-like genes, respectively. The VF-like genes encoding the type 4 fimbrial biogenesis protein PilB (VFDB ID: VFG000112), chemotaxis two-component response regu-

**Table 2.** **Differential phenotypic characteristics of strain H21R20$^T$, strain H23M41$^T$, *L. concretionis* Ko07$^T$, and *L. enzymogenes* 495$^T$**
Strains: 1, strain H21R20$^T$; 2, strain H23M41$^T$; 3, *L. concretionis* Ko07$^T$; 4, *L. enzymogenes* 495$^T$. All data except those for *L. enzymogenes* 495$^T$ (Srinivasan *et al.*, 2010) were obtained from this study. +, positive; –, negative; nd, not determined.

| Characteristic | 1 | 2 | 3 | 4 |
|---|---|---|---|---|
| Biochemical characteristics: | | | | |
| Nitrate reduction | – | – | + | – |
| Enzymatic activities of: | | | | |
| β-Glucosidase | + | + | + | – |
| Esterase lipase (C8) | + | + | – | + |
| Esterase (C4) | + | – | – | – |
| Crystine arylamidase, trypsin, α-galactosidase, β-Galactosidase, *N*-acetyl-β-glucosaminidase | – | – | – | + |
| Utilization as a sole carbon source: | | | | |
| L-Aspartic acid | + | – | + | nd |
| Glycyl-L-proline | + | – | + | nd |
| β-Hydroxy-D,L-butyric acid | – | – | + | nd |
| Propionic acid | – | – | + | nd |
| Citric acid, gentiobiose, sucrose, maltose, trehalose, turanose, melibiose, D-mannose | – | – | – | + |
| Chemical tolerance: | | | | |
| 1% Sodium lactate | + | + | – | nd |
| Tetrazolium blue | – | + | + | nd |
| Potassium tellurite | – | + | – | nd |
| D-Serine | + | – | – | nd |
| Troleandomycin | + | – | – | nd |

lator CheY1 (VFG002532), and short chain dehydrogenase/reductase family oxidoreductase (VFG038839) were only discovered in strain H21R20$^T$ and a gene encoding cyclic beta 1-2 glucan synthetase (VFG002219) was only found in strain H23M41$^T$ (Supplementary data Table S5). There were 58 and 61 gene clusters annotated as CAZymes in strains H21R20$^T$ and H23M41$^T$, respectively. All the compared *Lysobacter* strains had more genes related to glycoside hydrolases and glycosyl transferases than those related to carbohydrate-binding modules and carbohydrate esterases (Supplementary data Table S6).

### Physiological, morphological, and biochemical characteristics

Cells of both strains were Gram-stain-negative, non-spore-forming, strictly aerobic, and rod-shaped. The detailed cell sizes are presented in the description section below. Both strains showed motility, while strain H23M41$^T$ was much less motile than strain H21R20$^T$. This difference corresponds to each morphological feature and COG annotation. Strain H21R20$^T$ harbored a flagellum, while strain H23M41$^T$ didn't contain any flagella. Strain H23M41$^T$ also had the lowest proportion of COG with genes related to cell motility (code N) (Supplementary data Table S4). The colonies of both strains were opaque yellow, smooth, and circular with an intact margin. Strain H21R20$^T$ grew on TSB at 10–30°C and pH 6–9 and in the presence of 0–8% (wt/vol) NaCl, with optimal growth being observed at 30°C and pH 8 and in the presence of 0.5–3% (wt/vol) NaCl. Strain H23M41$^T$ grew at 10–30°C and pH 6–9 and in the presence of 0–5% (wt/vol) NaCl, with optimal growth being occurred at 30°C and pH 7–8 and in the presence of 0–3% (wt/vol) NaCl. Both strains grew well on TSA, MA, and R2A. The different phenotypic characteristics of the strains are shown in Table 2. All strains were positive for the following: oxidase and catalase, utilization of acetoacetic acid, tween 40, gelatin, glucuronamide, acetic acid, and L-glutamic acid as a sole carbon source (Biolog GEN III), and enzymatic activities of alkaline phosphatase, naphthol-AS-BI-phosphohydrolase, leucine arylamidase, acid phosphatase, β-glucosidase, and protease (API ZYM, 20NE). All strains were tolerant to the sodium butyrate, lincomycin, and lithium chloride (Biolog GEN III). All strains were negative for the following: utilization of dextrin, D-cellobiose, stachyose, D-raffinose, α-D-lactose, β-methyl-D-glucoside, D-salicin, *N*-acetyl-D-glucosamine, *N*-acetyl-β-D-mannosamine, *N*-acetyl-D-galactosamine, *N*-acetyl neuraminic acid, α-D-glucose, D-fructose, D-galactose, 3-methyl glucose, D-fucose, L-fucose, L-rhamnose, inosine, D-sorbitol, D-mannitol, D-arabitol, myo-inositol, glycerol, D-glucose-6-PO4, D-fructose-6-PO4, D-aspartic acid, D-serine, L-alanine, L-arginine, L-pyroglutamic acid, L-serine, pectin, D-galacturonic acid, L-galactonic acid lactone, D-gluconic acid, D-glucuronic acid, mucic acid, quinic acid, D-saccharic acid, *p*-hydroxy-phenylacetic acid, methyl pyruvate, D-lactic acid methyl ester, L-lactic acid, α-keto-glutaric acid, D-malic acid, L-malic acid, bromo-succinic acid, γ-amino-butryic acid, α-hydroxy-butyric acid, α-keto-butyric acid, L-histidine, and formic acid as a sole carbon source (Biolog GEN III), enzymatic activities of lipase (C14), α-chymotrypsin, β-glucuronidase, β-glucosidase, α-glucosidase, β-glucosidase, α-mannosidase, α-fucosidase, valine arylamidase, arginine dihydrolase, and urease (API ZYM, 20NE), indole production, and glucose fermentation (API 20NE). All strains were not tolerant to the fusidic acid, rifamycin SV, minocycline, guanidine HCl, niaproof 4, tetrazolium violet, and sodium bromate (Biolog GEN III). We tested the susceptibilities of the strains to 28 different types of antibiotics and these results are shown in Supplementary data Table S7. Of the three strains, only strain H21R20$^T$ showed resistance to tetracycline and tigecycline, while only strain H23M41$^T$ showed resistance to carbenicillin, azithromycin, and rifampicin. Strains H21R20$^T$ and H23M41$^T$ showed comparatively weak antibiotic susceptibilities than *L. concretionis* Ko07$^T$.

### Chemotaxonomic features

The major cellular fatty acids (> 10%) in both strains were iso-$C_{15:0}$ (23.9% for strain H21R20$^T$ and 26.4% for strain H23M41$^T$), iso-$C_{16:0}$ (13.7% and 11.5%), and summed feature 9 (iso-$C_{17:1}$ ω9c and/or $C_{16:0}$ 10-methyl) (26.5% and 28.6%), while those in *L. concretionis* Ko07$^T$ were iso-$C_{15:0}$ (34.4%) and summed feature 9 (28.0%) and those in *L. enzymogenes* 495$^T$ were iso-$C_{15:0}$ (44.4%) and iso-$C_{17:1}$ ω9c (13.9%) (Table 3). Strains H21R20$^T$ and H23M41$^T$ obtained DPG, PG, PE, and an unidentified phospholipid (Supplementary data Fig. S2). Both strains contained ubiquinone Q-8 as a major quinone (Supplementary data Fig. S3).

Taken together, strains H21R20$^T$ and H23M41$^T$ were both

**Table 3. Composition of cellular fatty acids (%) in strain H21R20$^T$, strain H23M41$^T$, *L. concretionis* Ko07$^T$, and *L. enzymogenes* 495$^T$**

Strains: 1, strain H21R20$^T$; 2, strain H23M41$^T$; 3, *L. concretionis* Ko07$^T$; 4, *L. enzymogenes* 495$^T$. All data were obtained from this study except *L. enzymogenes* 495$^T$ (Srinivasan *et al.*, 2010). The fatty acids that comprised < 1.0% of the total fatty acid content in all species were omitted. Symbol: tr, trace (< 1.0%); –, not detected.

| Cellular fatty acid (%) | 1 | 2 | 3 | 4 |
|---|---|---|---|---|
| **Saturated straight-chain** | | | | |
| $C_{16:0}$ | 4.0 | 4.9 | 4.3 | 4.5 |
| **Saturated branched-chain** | | | | |
| iso-$C_{11:0}$ | 4.9 | 4.5 | 5.3 | 8.1 |
| iso-$C_{14:0}$ | tr | tr | tr | tr |
| iso-$C_{15:0}$ | 23.9 | 26.4 | 34.4 | 44.4 |
| iso-$C_{16:0}$ | 13.7 | 11.5 | 3.8 | tr |
| iso-$C_{17:0}$ | 8.9 | 6.7 | 8.2 | 8.7 |
| anteiso-$C_{15:0}$ | 2.1 | 1.5 | 1.2 | tr |
| anteiso-$C_{17:0}$ | 1.3 | tr | tr | – |
| iso-$C_{11:0}$ 3OH | 6.1 | 5.6 | 6.4 | 8.7 |
| cyclo-$C_{17:0}$ | 1.1 | tr | tr | – |
| **Unsaturated branched-chain** | | | | |
| iso-$C_{15:1}$ F | 1.1 | 2.0 | 2.2 | – |
| iso-$C_{15:1}$ ω9c | – | – | – | 2.0 |
| iso-$C_{17:1}$ ω9c | – | – | – | 13.9 |
| $C_{16:1}$ ω7c alcohol | – | – | – | 1.1 |
| **Summed features** | | | | |
| 3 | 4.2 | 4.3 | 3.3 | 3.1 |
| 9 | 26.5 | 28.6 | 28.0 | – |

*Summed features were used when two or three fatty acids could not be separated using the Microbial Identification System. Summed feature 3 was comprised of $C_{16:1}$ ω7c and/or $C_{16:1}$ ω6c. Summed feature 9 was comprised of iso-$C_{17:1}$ ω9c and/or $C_{16:0}$ 10-methyl.

Gram-stain-negative and aerobic rods, and both strains contained various iso-branched fatty acids, ubiquinone Q-8, DPG, PG, and PE as observed in other *Lysobacter* species. However, the two strains showed clear distinctions in OGRIs and some differences in phenotypic and genomic features compared to *L. concretionis* Ko07$^T$ or *L. enzymogenes* 495$^T$. Therefore, we propose two novel strains, H21R20$^T$ and H23M41$^T$, as new members of the genus *Lysobacter*. We propose the name *L. ciconiae* sp. nov. for strain H21R20$^T$ and *L. avium* sp. nov. for strain H23M41$^T$.

**Description of *Lysobacter ciconiae* sp. nov.**

*Lysobacter ciconiae* (ci.co'ni.ae. N.L. gen. fem. n. *ciconiae* of a white stork).

Cells are Gram-stain-negative, non-spore-forming, strictly aerobic, mesophilic, motile, and rod-shaped (0.5–0.8 μm × 0.9–2.1 μm) with a flagellum. Colonies cultured for 48 h on TSA at 30°C are yellow, opaque, circular, smooth, and convex and have an intact margin. Cells grow at 10–30°C and pH 6–9 and in the presence of 0–8% (wt/vol) NaCl. Optimal growth occurs at 30°C and pH 8 and in the presence of 0.5–3% (wt/vol) NaCl. Cells are positive for oxidase and catalase activities, and utilize acetic acid, tween 40, L-aspartic acid, glucuronamide, glycyl-L-proline, gelatin, and L-glutamic acid as the sole carbon source (Biolog GEN III). Cells are tolerant to lithium chloride (Biolog GEN III) and are positive for esterase lipase (C8), esterase (C4), alkaline phosphatase, naphthol-AS-BI-phosphohydrolase, leucine arylamidase, acid phosphatase, β-glucosidase, and protease activities (API ZYM, 20NE). Cells are unable to utilize acetoacetic acid, β-hydroxy-D,L-butyric acid, propionic acid, L-histidine, dextrin, D-maltose, D-trehalose, D-cellobiose, gentiobiose, sucrose, D-turanose, stachyose, D-raffinose, α-D-lactose, D-melibiose, β-methyl-D-glucoside, D-salicin, *N*-acetyl-D-glucosamine, *N*-acetyl-β-D-mannosamine, *N*-acetyl-D-galactosamine, *N*-acetyl neuraminic acid, α-D-glucose, D-mannose, D-fructose, D-galactose, 3-methyl glucose, D-fucose, L-fucose, L-rhamnose, inosine, D-sorbitol, D-mannitol, D-arabitol, myo-inositol, glycerol, D-glucose-6-PO4, D-fructose-6-PO4, D-aspartic acid, D-serine, L-alanine, L-arginine, L-pyroglutamic acid, L-serine, pectin, D-galacturonic acid, L-galactonic acid lactone, D-gluconic acid, D-glucuronic acid, mucic acid, quinic acid, D-saccharic acid, *p*-hydroxy-phenylacetic acid, methyl pyruvate, D-lactic acid methyl ester, L-lactic acid, citric acid, α-keto-glutaric acid, D-malic acid, L-malic acid, bromo-succinic acid, γ-amino-butryic acid, α-hydroxy-butyric acid, α-keto-butyric acid, and formic acid as a sole carbon source (Biolog GEN III). Cells are not tolerant to tetrazolium blue, potassium tellurite, sodium butyrate, lincomycin, 1% sodium lactate, D-serine, troleandomycin, fusidic acid, rifamycin SV, minocycline, guanidine HCl, niaproof 4, tetrazolium violet, and sodium bromate (Biolog GEN III). Cells are also negative for lipase (C14), crystine arylamidase, α-chymotrypsin, α-galactosidase, β-glucuronidase, α-glucosidase, *N*-acetyl-β-glucosaminidase, α-mannosidase, α-fucosidase, trypsin, valine arylamidase, arginine dihydrolase, urease, and β-galactosidase activities (API ZYM, 20NE), nitrate reduction, indole production and glucose fermentation (API 20NE). The major cellular fatty acids are iso- $C_{15:0}$, iso-$C_{16:0}$, and summed feature 9 (iso-$C_{17:1}$ ω9c and/or $C_{16:0}$ 10-methyl), while a major quinone is ubiquinone Q-8. The major polar lipids are DPG, PG, and PE.

Type strain H21R20$^T$ (= KCTC 82316$^T$ = JCM 34832$^T$) was isolated from the faeces of the Oriental stork *Ciconia boyciana*. The DDBJ/ENA/GenBank accession numbers for the 16S rRNA gene sequence and genome sequence of strain H21R20$^T$ are MT764981 and CP063656, respectively. The G + C content of the genomic DNA is 67.3%.

**Description of *Lysobacter avium* sp. nov.**

*Lysobacter avium* (a'vi.um. N.L. gen. pl. n. *avium* of birds).

Cells are Gram-stain-negative, non-spore-forming, strictly aerobic, mesophilic, weakly motile, and rod-shaped (0.5–0.8 μm × 1.0–3.5 μm). Colonies cultured for 48 h on TSA at 30°C are yellow, opaque, circular, smooth, and convex and have an intact margin. Cells grow at 10–30°C and pH 6–9 and in the presence of 0–5% (wt/vol) NaCl. Optimal growth occurs at 30°C and pH 7–8 and in the presence of 0–3% (wt/vol) NaCl. Cells are positive for oxidase and catalase, and utilize acetoacetic acid, tween 40, gelatin, glucuronamide, acetic acid, and L-glutamic acid as the sole carbon source (Biolog GEN III). Cells are tolerant to 1% sodium lactate, tetrazolium blue, potassium tellurite, sodium butyrate, lincomycin, and lithium chloride (Biolog GEN III), and are positive for esterase lipase (C8), alkaline phosphatase, naphthol-AS-BI-phosphohydrolase, leucine arylamidase, acid phosphatase, β-glucosidase, and protease activities (API ZYM, 20NE). Cells are unable to utilize L-aspartic acid, glycyl-L-proline, β-hydroxy-D,L-butyric acid, propionic acid, dextrin, D-maltose, D-trehalose, D-cellobiose, gentiobiose, sucrose, D-turanose, stachyose, D-raffinose, α-D-lactose, D-melibiose, β-methyl-D-glucoside, D-salicin, *N*-acetyl-D-glucosamine, *N*-acetyl-β-D-mannosamine, *N*-acetyl-D-galactosamine, *N*-acetyl neuraminic acid, α-D-glucose, D-mannose, D-fructose, D-galactose, 3-methyl glucose, D-fucose, L-fucose, L-rhamnose, inosine, D-sorbitol, D-mannitol, D-arabitol, myo-inositol, glycerol, D-glucose-6-PO4, D-fructose-6-PO4, D-aspartic acid, D-serine, L-alanine, L-arginine, L-pyroglutamic acid, L-serine, pectin, D-galacturonic acid, L-galactonic acid lactone, D-gluconic acid, D-glucuronic acid, mucic acid, quinic acid, D-saccharic acid, *p*-hydroxy-phenylacetic acid, methyl pyruvate, D-lactic acid methyl ester, L-lactic acid, citric acid, α-keto-glutaric acid, D-malic acid, L-malic acid, bromo-succinic acid, γ-amino-butryic acid, α-hydroxy-butyric acid, α-keto-butyric acid, L-histidine, and formic acid as the sole carbon source (Biolog GEN III). Cells are not tolerant to D-serine, troleandomycin, fusidic acid, rifamycin SV, minocycline, guanidine HCl, niaproof 4, tetrazolium violet, and sodium bromate (Biolog GEN III). Cells are negative for lipase (C14), crystine arylamidase, α-chymotrypsin, α-galactosidase, β-glucuronidase, α-glucosidase, *N*-acetyl-β-glucosaminidase, α-mannosidase, α-fucosidase, trypsin, esterase (C4), valine arylamidase, arginine dihydrolase, urease, and β-galactosidase activities (API ZYM, 20NE), indole production, nitrate reduction, and glucose fermentation (API 20NE). The major cellular fatty acids are iso-$C_{15:0}$, iso-$C_{16:0}$, and summed feature 9 (iso-$C_{17:1}$ ω9c and/or $C_{16:0}$ 10-methyl), while a major quinone is ubiquinone Q-8. The major polar lipids are DPG, PG, and PE.

Type strain H23M41$^T$ (= KCTC 62676$^T$ = JCM 33223$^T$) was

isolated from the faeces of the Oriental stork *Ciconia boyciana*. The DDBJ/ENA/GenBank accession numbers for the 16S rRNA gene sequence and genome sequence of strain H23M41$^T$ are MT764977 and CP063657, respectively. The G + C content of the genomic DNA is 66.6%.

## Acknowledgements

This work was supported by grants from the Mid-Career Researcher Program (NRF-2020R1A2C3012797) through the National Research Foundation of Korea (NRF) and the National Institute of Biological Resources (NIBR201801106) funded by the Ministry of Environment of Korea (MOE). This work was also supported by the NRF grant funded by the Korean government (MSIT) (No. NRF-2018R1A5A1025077).

## Conflicts of Interest

The authors declare that there are no conflicts of interest.

## Ethical Statement

All sampling conducted in this study was approved by the Institutional Animal Care and Use Committee of Kyung Hee University (Permit number: KHUASP(SE)-18-048) and complied with the guidelines of the Committee.

## References

**Arkin, A.P., Cottingham, R.W., Henry, C.S., Harris, N.L., Stevens, R.L., Maslov, S., Dehal, P., Ware, D., Perez, F., Canon, S., *et al.*** 2018. KBase: the United States department of energy systems biology knowledgebase. *Nat. Biotechnol.* **36**, 566–569.

**Brettin, T., Davis, J.J., Disz, T., Edwards, R.A., Gerdes, S., Olsen, G.J., Olson, R., Overbeek, R., Parrello, B., Pusch, G.D., *et al.*** 2015. *RASTtk*: a modular and extensible implementation of the RAST algorithm for building custom annotation pipelines and annotating batches of genomes. *Sci. Rep.* **5**, 8365.

**Chen, I.M.A., Chu, K., Palaniappan, K., Pillay, M., Ratner, A., Huang, J., Huntemann, M., Varghese, N., White, J.R., Seshadri, R., *et al.*** 2019. IMG/M v. 5.0: an integrated data management and comparative analysis system for microbial genomes and microbiomes. *Nucleic Acids Res.* **47**, D666–D677.

**Chhetri, G., Kim, J., Kim, I., and Seo, T.** 2019. *Lysobacter caseinilyticus*, sp. nov., a casein hydrolyzing bacterium isolated from sea water. *Antonie van Leeuwenhoek* **112**, 1349–1356.

**Chin, C.S., Alexander, D.H., Marks, P., Klammer, A.A., Drake, J., Heiner, C., Clum, A., Copeland, A., Huddleston, J., Eichler, E.E., *et al.*** 2013. Nonhybrid, finished microbial genome assemblies from long-read SMRT sequencing data. *Nat. Methods* **10**, 563–569.

**Choi, H., Im, W.T., and Park, J.S.** 2018. *Lysobacter spongiae* sp. nov., isolated from spongin. *J. Microbiol.* **56**, 97–103.

**Christensen, P. and Cook, F.D.** 1978. *Lysobacter*, a new genus of nonfruiting, gliding bacteria with a high base ratio. *Int. J. Syst. Evol. Microbiol.* **28**, 367–393.

**Chun, J., Oren, A., Ventosa, A., Christensen, H., Arahal, D.R., da Costa, M.S., Rooney, A.P., Yi, H., Xu, X.W., De Meyer, S., *et al.*** 2018. Proposed minimal standards for the use of genome data for the taxonomy of prokaryotes. *Int. J. Syst. Evol. Microbiol.* **68**, 461–466.

**Collins, M.D. and Jones, D.** 1981. Distribution of isoprenoid quinone structural types in bacteria and their taxonomic implication. *Microbiol. Rev.* **45**, 316–354.

**Du, J., Singh, H., Ngo, H.T.T., Won, K.H., Kim, K.Y., and Yi, T.H.** 2015. *Lysobacter tyrosinelyticus* sp. nov. isolated from Gyeryongsan national park soil. *J. Microbiol.* **53**, 365–370.

**Fang, B.Z., Xie, Y.G., Zhou, X.K., Zhang, X.T., Liu, L., Jiao, J.Y., Xiao, M., and Li, W.J.** 2020. *Lysobacter prati* sp. nov., isolated from a plateau meadow sample. *Antonie van Leeuwenhoek* **113**, 763–772.

**Felsenstein, J.** 1981. Evolutionary trees from DNA sequences: a maximum likelihood approach. *J. Mol. Evol.* **17**, 368–376.

**Ha, S.M., Kim, C.K., Roh, J., Byun, J.H., Yang, S.J., Choi, S.B., Chun, J., and Yong, D.** 2019. Application of the whole genome-based bacterial identification system, TrueBac ID, using clinical isolates that were not identified with three matrix-assisted laser desorption/ionization time-of-flight mass spectrometry (MALDI-TOF MS) systems. *Ann. Lab. Med.* **39**, 530–536.

**Hiraishi, A., Ueda, Y., Ishihara, J., and Mori, T.** 1996. Comparative lipoquinone analysis of influent sewage and activated sludge by high-performance liquid chromatography and photodiode array detection. *J. Gen. Appl. Microbiol.* **42**, 457–469.

**Huo, Y., Kang, J.P., Hurh, J., Han, Y., Ahn, J.C., Mathiyalagan, R., Piao, C., and Yang, D.C.** 2018. *Lysobacter panacihumi* sp. nov., isolated from ginseng cultivated soil. *J. Microbiol.* **56**, 748–752.

**Hyun, D.W., Sung, H., Kim, P.S., Yun, J.H., and Bae, J.W.** 2021. *Leucobacter coleopterorum* sp. nov., *Leucobacter insecticola* sp. nov., and *Leucobacter viscericola* sp. nov., isolated from the intestine of the diving beetles, *Cybister brevis* and *Cybister lewisianus*, and emended description of the genus *Leucobacter*. *J. Microbiol.* **59**, 360–368.

**Im, W.T., Siddiqi, M.Z., Kim, S.Y., Huq, M.A., Lee, J.H., and Choi, K.D.** 2020. *Lysobacter lacus* sp. nov., isolated from from lake sediment. *Int. J. Syst. Evol. Microbiol.* **70**, 2211–2216.

**Jang, J.H., Lee, D., and Seo, T.** 2018. *Lysobacter pedocola* sp. nov., a novel species isolated from Korean soil. *J. Microbiol.* **56**, 387–392.

**Jeong, S.E., Lee, H.J., and Jeon, C.O.** 2016. *Lysobacter aestuarii* sp. nov., isolated from estuary sediment. *Int. J. Syst. Evol. Microbiol.* **66**, 1346–1351.

**Kim, S.J., Ahn, J.H., Weon, H.Y., Hong, S.B., Seok, S.J., Kim, J.S., and Kwon, S.W.** 2016. *Lysobacter terricola* sp. nov., isolated from greenhouse soil. *Int. J. Syst. Evol. Microbiol.* **66**, 1401–1406.

**Kim, S.J., Ahn, J.H., Weon, H.Y., Joa, J.H., Hong, S.B., Seok, S.J., Kim, J.S., and Kwon, S.W.** 2017. *Lysobacter solanacearum* sp. nov., isolated from rhizosphere of tomato. *Int. J. Syst. Evol. Microbiol.* **67**, 1102–1106.

**Kim, I., Choi, J., Chhetri, G., and Seo, T.** 2019. *Lysobacter helvus* sp. nov. and *Lysobacter xanthus* sp. nov., isolated from soil in South Korea. *Antonie van Leeuwenhoek* **112**, 1253–1262.

**Kim, K.R., Kim, K.H., Khan, S.A., Kim, H.M., Han, D.M., and Jeon, C.O.** 2021. *Lysobacter arenosi* sp. nov. and *Lysobacter solisilvae* sp. nov. isolated from soil. *J. Microbiol.* **59**, 709–717.

**Kluge, A.G. and Farris, J.S.** 1969. Quantitative phyletics and the evolution of anurans. *Syst. Biol.* **18**, 1–32.

**Kumar, S., Stecher, G., and Tamura, K.** 2016. MEGA7: molecular evolutionary genetics analysis version 7.0 for bigger datasets. *Mol. Biol. Evol.* **33**, 1870–1874.

**Lane, D.** 1991. 16S/23S rRNA sequencing. *In* Stackebrandt, E. and Goodfellow, M. (eds.), Nucleic Acid Techniques in Bacterial Systematics. pp. 115–175. John Wiley and Sons, New York, USA.

**Lee, D., Jang, J.H., Cha, S., and Seo, T.** 2017. *Lysobacter humi* sp. nov., isolated from soil. *Int. J. Syst. Evol. Microbiol.* **67**, 951–955.

**Lee, S.Y., Kang, W., Kim, P.S., Kim, H.S., Sung, H., Shin, N.R., Whon, T.W., Yun, J.H., Lee, J.Y., Lee, J.Y., *et al.*** 2019. *Undibacterium piscinae* sp. nov., isolated from Korean shiner intestine. *Int. J.*

*Syst. Evol. Microbiol.* **69**, 3148–3154.
**Lee, S.Y., Kang, W., Kim, P.S., Kim, H.S., Sung, H., Shin, N.R., Yun, J.H., Lee, J.Y., Lee, J.Y., Jung, M.J., *et al.*** 2020. *Jeotgalibaca ciconiae* sp. nov., isolated from the faeces of an Oriental stork. *Int. J. Syst. Evol. Microbiol.* **70**, 3247–3254.
**Lee, I., Kim, Y.O., Park, S.C., and Chun, J.** 2016. OrthoANI: an improved algorithm and software for calculating average nucleotide identity. *Int. J. Syst. Evol. Microbiol.* **66**, 1100–1103.
**Lee, S.Y., Sung, H., Kim, P.S., Kim, H.S., Lee, J.Y., Lee, J.Y., Jeong, Y.S., Tak, E.J., Han, J.E., Hyun, D.W., *et al.*** 2021. Description of *Ornithinimicrobium ciconiae* sp. nov., and *Ornithinimicrobium avium* sp. nov., isolated from the faeces of the endangered and near-threatened birds. *J. Microbiol.* **59**, 978–987.
**Li, W., Elderiny, N.S., Ten, L.N., Lee, S.Y., Kim, M.K., and Jung, H.Y.** 2020. *Lysobacter terrigena* sp. nov., isolated from a Korean soil sample. *Arch. Microbiol.* **202**, 637–643.
**Li, L., Stoeckert, C.J.Jr, and Roos, D.S.** 2003. OrthoMCL: identification of ortholog groups for eukaryotic genomes. *Genome Res.* **13**, 2178–2189.
**Luo, Y., Dong, H., Zhou, M., Huang, Y., Zhang, H., He, W., Sheng, H., and An, L.** 2019. *Lysobacter psychrotolerans* sp. nov., isolated from soil in the Tianshan Mountains, Xinjiang, China. *Int. J. Syst. Evol. Microbiol.* **69**, 926–931.
**Margesin, R., Zhang, D.C., Albuquerque, L., Froufe, H.J., Egas, C., and da Costa, M.S.** 2018. *Lysobacter silvestris* sp. nov., isolated from alpine forest soil, and reclassification of *Luteimonas tolerans* as *Lysobacter tolerans* comb. nov. *Int. J. Syst. Evol. Microbiol.* **68**, 1571–1577.
**Meier-Kolthoff, J.P., Auch, A.F., Klenk, H.P., and Göker, M.** 2013. Genome sequence-based species delimitation with confidence intervals and improved distance functions. *BMC Bioinformatics* **14**, 60.
**Minnikin, D.E., O'donnell, A.G., Goodfellow, M., Alderson, G., Athalye, M., Schaal, A., and Parlett, J.H.** 1984. An integrated procedure for the extraction of bacterial isoprenoid quinones and polar lipids. *J. Microbiol. Methods* **2**, 233–241.
**Na, S.I., Kim, Y.O., Yoon, S.H., Ha, S.M., Baek, I., and Chun, J.** 2018. UBCG: Up-to-date bacterial core gene set and pipeline for phylogenomic tree reconstruction. *J. Microbiol.* **56**, 280–285.
**Parte, A.C., Carbasse, J.S., Meier-Kolthoff, J.P., Reimer, L.C., and Göker, M.** 2020. List of Prokaryotic names with Standing in Nomenclature (LPSN) moves to the DSMZ. *Int. J. Syst. Evol. Microbiol.* **70**, 5607–5612.
**Price, M.N., Dehal, P.S., and Arkin, A.P.** 2009. FastTree: computing large minimum evolution trees with profiles instead of a distance matrix. *Mol. Biol. Evol.* **26**, 1641–1650.
**Saitou, N. and Nei, M.** 1987. The neighbor-joining method: a new method for reconstructing phylogenetic trees. *Mol. Biol. Evol.* **4**, 406–425.
**Sasser, M.** 1990. Identification of bacteria by gas chromatography of cellular fatty acids. MIDI Technical Note 101. MIDI Inc., Newark, Delaware, USA.
**Schaeffer, A.B. and Fulton, M.D.** 1933. A simplified method of staining endospores. *Science* **77**, 194.
**Siddiqi, M.Z. and Im, W.T.** 2016. *Lysobacter hankyongensis* sp. nov., isolated from activated sludge and *Lysobacter sediminicola* sp. nov., isolated from freshwater sediment. *Int. J. Syst. Evol. Microbiol.* **66**, 212–218.
**Singh, H., Du, J., Ngo, H.T.T., Won, K.H., Yang, J.E., Kim, K.Y., and Yi, T.H.** 2015a. *Lysobacter fragariae* sp. nov. and *Lysobacter rhizosphaerae* sp. nov. isolated from rhizosphere of strawberry plant. *Antonie van Leeuwenhoek* **107**, 1437–1444.
**Singh, H., Du, J., Won, K.H., Yang, J.E., Akter, S., Kim, K.Y., and Yi, T.H.** 2015b. *Lysobacter novalis* sp. nov., isolated from fallow farmland soil. *Int. J. Syst. Evol. Microbiol.* **65**, 3131–3136.
**Srinivasan, S., Kim, M.K., Sathiyaraj, G., Kim, H.B., Kim, Y.J., and Yang, D.C.** 2010. *Lysobacter soli* sp. nov., isolated from soil of a ginseng field. *Int. J. Syst. Evol. Microbiol.* **60**, 1543–1547.
**Ten, L.N., Jeon, J., Elderiny, N.S., Kim, M.K., Lee, S.Y., and Jung, H.Y.** 2020. *Lysobacter segetis* sp. nov., isolated from soil. *Curr. Microbiol.* **77**, 166–172.
**Ten, L.N., Jung, H.M., Im, W.T., Yoo, S.A., and Lee, S.T.** 2008. *Lysobacter daecheongensis* sp. nov., isolated from sediment of stream near the Daechung dam in South Korea. *J. Microbiol.* **46**, 519–524.
**Thompson, J.D., Higgins, D.G., and Gibson, T.J.** 1994. CLUSTAL W: improving the sensitivity of progressive multiple sequence alignment through sequence weighting, position-specific gap penalties and weight matrix choice. *Nucleic Acids Res.* **22**, 4673–4680.
**Xiao, M., Zhou, X.K., Chen, X., Duan, Y.Q., Alkhalifah, D.H.M., Im, W.T., Hozzein, W.N., Chen, W., and Li, W.J.** 2019. *Lysobacter tabacisoli* sp. nov., isolated from rhizosphere soil of *Nicotiana tabacum* L. *Int. J. Syst. Evol. Microbiol.* **69**, 1875–1880.
**Xu, J., Sheng, M., Yang, Z., Qiu, J., Zhang, J., Zhang, L., and He, J.** 2021. *Lysobacter gilvus* sp. nov., isolated from activated sludge. *Arch. Microbiol.* **203**, 7–11.
**Ye, X.M., Chu, C.W., Shi, C., Zhu, J.C., He, Q., and He, J.** 2015. *Lysobacter caeni* sp. nov., isolated from the sludge of a pesticide manufacturing factory. *Int. J. Syst. Evol. Microbiol.* **65**, 845–850.
**Zhang, L., Bai, J., Wang, Y., Wu, G.L., Dai, J., and Fang, C.X.** 2011. *Lysobacter korlensis* sp. nov. and *Lysobacter bugurensis* sp. nov., isolated from soil. *Int. J. Syst. Evol. Microbiol.* **61**, 2259–2265.
**Zhang, X.J., Yao, Q., Wang, Y.H., Yang, S.Z., Feng, G.D., and Zhu, H.H.** 2019. *Lysobacter silvisoli* sp. nov., isolated from forest soil. *Int. J. Syst. Evol. Microbiol.* **69**, 93–98.
**Zhang, H., Yohe, T., Huang, L., Entwistle, S., Wu, P., Yang, Z., Busk, P.K., Xu, Y., and Yin, Y.** 2018. dbCAN2: a meta server for automated carbohydrate-active enzyme annotation. *Nucleic Acids Res.* **46**, W95–W101.